Isotope dependence of the lattice parameter of germanium from path-integral Monte Carlo simulations

José C. Noya, Carlos P. Herrero, and Rafael Ramírez
Instituto de Ciencia de Materiales, Consejo Superior de Investigaciones Científicas (CSIC), Campus Cantoblanco, 28049 Madrid, Spain
(Received 1 October 1996)

The dependence of the lattice parameter upon the isotope mass for five isotopically pure Ge crystals was studied by quantum path-integral Monte Carlo simulations. The interatomic interactions in the solid were described by an empirical potential of the Stillinger-Weber type. At 50 K the isotopic effect leads to an increase of 2.3×10^{-4} Å in the lattice parameter of ^{70}Ge with respect to ^{76}Ge. Comparison of the simulation results with available experimental data for ^{74}Ge shows that the employed model provides a realistic description of this anharmonic effect. The path-integral results were compared to those derived from a quasiharmonic approximation of the crystal. Within this approximation, the calculated fractional change of the lattice parameter of ^{74}Ge with respect to a crystal whose atoms have the average mass of natural Ge amounts to $\Delta a/a=-9.2\times10^{-6}$ at $T=0$ K. Some limitations of the quasiharmonic approximation are shown at temperatures above 200 K. [S0163-1829(97)01725-6]

I. INTRODUCTION

The availability of isotopically pure crystals with low carrier and impurity concentrations has allowed in the last years the investigation of isotope effects on lattice dynamical and electronic properties of semiconductors.[1] Due to zero-point motion, the atoms in a solid feel the anharmonicity of the interatomic potentials even at low temperatures. Therefore, the lattice parameters of two chemically identical crystals formed by different isotopes do not coincide,[1–7] heavier isotopes having smaller zero-point delocalization (as expected in a harmonic approximation) and smaller lattice parameters (an anharmonic effect). Moreover, phonon-related properties, such as thermal expansion or melting temperature, are expected to depend on the isotope mass.

In this context, the existence of mass differences in the isotope distribution in the natural materials causes a translational-symmetry breaking, which affects crystal properties such as the phonon spectrum (phonon energy shifts and band broadenings) and the atomic hopping mobility. These effects have been studied by different experimental techniques on germanium[5,7–9] and diamond[6,10–12] single crystals, either isotopically pure or intentionally disordered with controlled isotope concentrations. Also, the study of order-disorder features in the phonon or electron states of a crystal via isotopes addresses questions such as the applicability of different theories to weak forms of disorder.[13]

This work is focused on the dependence upon the isotope mass of the lattice parameter in isotopically pure Ge crystals. The germanium isotopes, their masses and relative natural abundance are shown in Table I. Since this isotope-mass effect is caused by the quantum nature of the atomic nuclei and the anharmonicity of the interaction potentials, a convenient approach to this question is the path-integral Monte Carlo (PIMC) method, that allows one to study finite-temperature properties of many-body systems without the simplifying assumption of harmonic potentials. In this line, path-integral MC simulations have been reported on isotope effects upon the lattice constant of solid neon (^{20}Ne and ^{22}Ne),[14] and on the melting curves of helium (^{4}He and ^{3}He).[15] An alternative approach to study anharmonic effects in solids is the so-called quasiharmonic approximation (QHA).[16] In this approximation, frequencies of the vibrational modes in a crystal are made volume dependent, and for given volume and temperature, the crystal is assumed to be harmonic.

The purpose of the present work is twofold: first, to obtain the change in lattice constant for different Ge isotopes by a many-body calculation (PIMC simulations), and second to check the validity of the QHA to describe the anharmonic effects which appear in crystals at finite temperatures. Thus, one can discriminate between anharmonic effects due to thermal expansion of the lattice (treated in the QHA by the renormalization of mode frequencies) and other effects, such as phonon-phonon interactions, not included in the QHA.[16]

We present several mass-related equilibrium properties of isotopically pure Ge crystals, derived from PIMC simulations in the isothermal-isobaric ensemble. The interatomic potentials are described by an empirical potential of the Stillinger-Weber (SW) type.[17–19] The reliability of this effective potential has been assessed by comparison of several calculated crystal properties (phonon dispersion curves, vibrational density of states, Grüneisen and elastic constants) to experimental data. The results obtained in the MC simulations for the lattice constant have been compared to x-ray

TABLE I. Stable isotopes of Ge and their relative abundance.

Isotope	Mass (amu)	Abundance
^{70}Ge	69.92	20.5%
^{72}Ge	71.92	27.4%
^{73}Ge	72.92	7.8%
^{74}Ge	73.92	36.5%
^{76}Ge	75.92	7.8%
Average, ^{av}Ge	72.63	

diffraction data for ^{74}Ge and to those obtained in a QHA with the same interatomic potential.

The paper is organized as follows. In Sec. II we describe the computational method (path-integral Monte Carlo and quasiharmonic approximation); the results and discussion are presented in Sec. III, and the paper closes with a summary (Sec. IV).

II. COMPUTATIONAL METHOD

A. Path-integral Monte Carlo

The path-integral Monte Carlo method is based on the evaluation of the partition function of a quantum system through a decomposition of its density matrix at a given temperature into P (Trotter number) density matrices, each one being evaluated at a higher temperature PT. Good reviews of the method can be found elsewhere.[20–22] The feasibility of the method relies on an isomorphism between the quantum system and a classical one, obtained by substitution of each quantum particle (i.e., atomic nucleus in the present context) by a cyclic chain of P classical particles (beads). We denote by j the index, running from 1 to P, that labels sequentially the beads of the cyclic chains. Interatomic interactions in the classical isomorph are then restricted to beads of different chains sharing the same label j. Moreover, a given bead j in a chain interacts harmonically with the beads $j-1$ and $j+1$ of the same chain with a spring constant κ given by

$$\kappa = MP/\beta^2\hbar^2, \tag{1}$$

where M is the mass of the quantum particle, $\beta=(k_BT)^{-1}$, and k_B is the Boltzmann constant. Although the isomorphism is exact in the limit $P\to\infty$, in practice very good approximations can be obtained at finite temperatures for moderate values of P.[23] In the classical limit, the cyclic chain collapses into a single point ($P=1$). Note that within the path-integral formalism, the dependence of the thermodynamic properties upon the particle mass M enters through the renormalization of the spring constant κ.

The simulation of c-Ge was performed on a $2\times2\times2$ supercell of the germanium face-centered-cubic (fcc) cell containing 64 Ge atoms, with periodic boundary conditions. We have checked that there is no significant difference in the calculated lattice parameters when the simulation cell is taken as a $3\times3\times3$ supercell. The Ge nuclei were treated as quantum particles interacting through an empirical SW-type potential (see below). Finite-temperature properties were derived from Metropolis Monte Carlo sampling.[20,24–26] A Monte Carlo step (MCS) consists of sequential moves of (i) the beads associated to each nucleus, (ii) the center of gravity of the cyclic chain associated to each nucleus, and (iii) the logarithm of the volume of the simulation cell.[27] After an initial equilibration of 5×10^4 MCS, the calculation of ensemble average properties was performed over 6×10^5 MCS. The simulations have been performed in a temperature range between 50 K and 600 K, and at constant pressure (1 atm). Natural germanium was modeled by setting a value for the atomic mass $M=72.63$ amu, corresponding to the average mass of natural germanium (^{av}Ge). The Trotter number P was made temperature dependent, and was taken as the integral number closest to $1600/T$. At temperatures higher than 400 K, we took $P=4$.

The interaction between germanium atoms was modeled by a potential proposed by Ding and Andersen,[17] slightly modified by Laradji *et al.*[18] to give a lattice parameter at 0 K closer to the experimental data. It has the analytical form of a SW potential,[19] where the set of potential parameters was adjusted to reproduce some experimental features of germanium, as the cohesive energy of the crystal at 0 K, the density and the elastic constants at atmospheric pressure, and the radial distribution function of amorphous germanium. This potential is not adequate to reproduce the properties of liquid germanium.[17]

B. Quasiharmonic approximation

In the quasiharmonic approximation, the anharmonicity is considered a weak effect and the phonon frequencies of the crystal are renormalized by taking into account the thermal expansion.[16] The vibrational free energy of a crystal of volume V and isotope mass M, at temperature T, is given by[28]

$$F(V,T,M)=U_0(V)+\sum_{\mathbf{q},i}\left(\frac{1}{2}\hbar\omega_i(\mathbf{q})+\frac{1}{2}k_BT\times\ln\{1-\exp[-\hbar\omega_i(\mathbf{q})/k_BT]\}\right), \tag{2}$$

where $U_0(V)$ is the the potential energy of the crystal with the atoms fixed at their equilibrium positions, $\mathbf{q}$ indicates a wave vector within the Brillouin zone (BZ) of the crystal, and i is the band index. The free energy depends implicitly on the isotope mass through the mass dependence of the phonon frequencies, $\omega_i(\mathbf{q})\propto M^{-1/2}$. The dependence of each phonon mode $\omega_i(\mathbf{q})$ on the crystal volume V is given by the Grüneisen constant $\gamma_i(\mathbf{q})$,[29] defined as:

$$\gamma_i(\mathbf{q})=-\frac{\partial[\ln ln\,\omega_i(\mathbf{q})]}{\partial(\ln V)}. \tag{3}$$

We have calculated the phonon frequencies of Ge by diagonalization of the dynamical matrix derived from the SW-type potential on a grid of 1140 wave vectors in the irreducible part of the BZ. The set of $\mathbf{q}$ points were chosen according to the method of Ref. 30. $F(V,T,M)$ was evaluated by means of Eq. (2) for a set of volumes and temperatures, and for each isotope mass. The equilibrium volume was then determined by the minimum of $F(V,T,M)$ as a function of V for fixed M and T. The same procedure was employed to evaluate the classical limit of the vibrational free energy within the QHA. The Grüneisen constants were determined from Eq. (3) by numerical differentiation.

III. RESULTS AND DISCUSSION

To characterize the interatomic potential employed in our simulations,[18] we have calculated the phonon dispersion curves, the phonon density of states, the Grüneisen constants, as well as the elastic constants and bulk modulus of an ^{av}Ge crystal. The phonon dispersion curves along several symmetry directions in the BZ are shown in Fig. 1. These

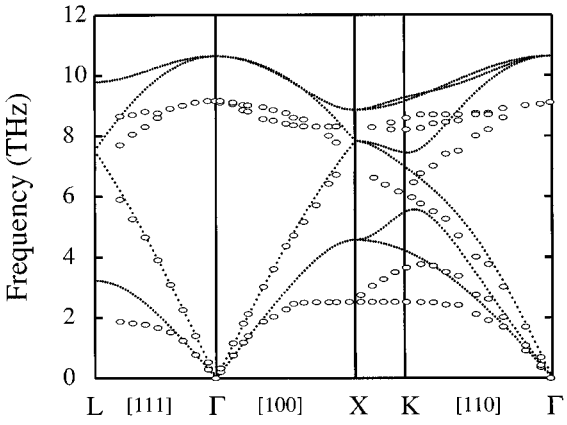

FIG. 1. Phonon dispersion curves of ^{av}Ge along several symmetry directions in the irreducible Brillouin zone. Dotted lines are results obtained from the SW-type potential. The experimental results (Ref. 31) are shown by open symbols.

curves are almost identical to those presented by Ding and Andersen,[17] who employed a potential slightly different from that used in the present work. The frequencies predicted for the optical modes are larger than the experimental values[17,31,32] by about 2 THz (67 cm^{-1}). The employed potential model reproduces well the dispersion of the acoustic modes near the Γ point. However, near the boundary of the BZ, the acoustic modes are found at higher frequencies than experimental modes. Ding and Andersen[17] showed that it is not possible to fit simultaneously the optical-phonon frequencies and the slopes of the acoustic branches near the Γ point, by means of a potential of the SW type.

The calculated phonon density of states of ^{av}Ge is displayed in Fig. 2, and compared to the data derived from inelastic neutron scattering.[32,33] The area of both curves is normalized to unity. The maxima of the acoustic and optical bands for the phonon density of states obtained from the SW-type potential are shifted with respect to the experimental curve by about 67 cm^{-1} toward higher frequencies.

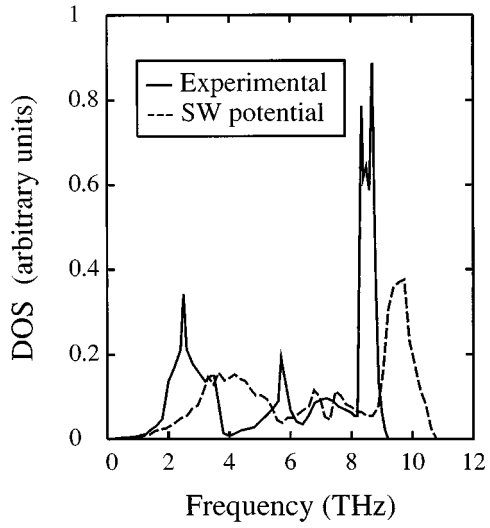

FIG. 2. Phonon density of states of ^{av}Ge. The solid line is derived from inelastic neutron scattering data (Ref. 33). The dashed line is the result for the SW-type potential.

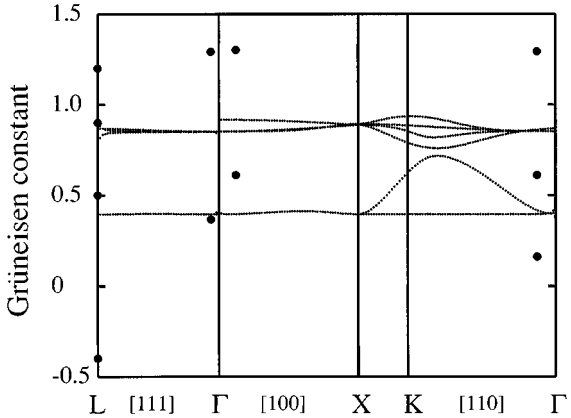

FIG. 3. Calculated Grüneisen constants of ^{av}Ge along several symmetry directions in the BZ. Black circles are experimental results (Ref. 31).

The calculated Grüneisen constants for the optical and acoustic modes of ^{av}Ge are shown in Fig. 3 along several directions in the BZ, and are compared to available experimental data.[31] The employed SW-type potential predicts Grüneisen constants for the optical modes that are about 0.35 lower than the experimental values.[5,34] The calculated Grüneisen constants for the acoustic modes amount to about 0.4 along the directions [100] and [111] in the BZ. The value found at the Γ point is in good agreement with the experiment. However, at the reciprocal point L, the experimental Grüneisen constant is negative (about -0.4). This negative value has important physical consequences for the thermal properties of the crystal, as it is the origin of the negative thermal expansion found for Ge at temperatures between 15 and 40 K.[35] The SW-type potential is unable to reproduce the negative thermal expansion of Ge, since it gives Grüneisen constants for the phonon modes that are always positive. In this context, it has been shown[36,37] that positive Grüneisen constants are obtained when the magnitude of noncentral forces (angular forces that stabilize the diamond structure) is dominant with respect to that of central forces. The SW-type potential overestimates the strength of angular forces, as it is not able to reproduce the negative thermal expansion of Ge. This deficiency of the SW potential has been already studied in a PIMC simulation of silicon.[27] In spite of the shortcomings of this kind of interatomic potential, it is much more suited for finite-temperature simulations of the crystal than other currently employed potentials, such as the Keating model potential,[38] which gives a negative linear thermal expansion at all temperatures.[18,39]

From the slope of the dispersion curves for the acoustic modes near the Γ point, we calculated the elastic constants and bulk modulus of ^{av}Ge at $T=0$.[40] At finite temperatures, these parameters were obtained within the QHA, by taking into account the mode-dependent Grüneisen constants $\gamma_i(\mathbf{q})$. The results are shown in Table II, along with the experimental data at 100 K and 300 K.[31,32] The deviation of the calculated values with respect to the experiment is about 5% for both the elastic constants and the bulk modulus. We have checked that the bulk modulus obtained at 0 K in the classical limit from the phonon dispersion curves agrees with

TABLE II. Calculated and experimental elastic constants and bulk modulus of ^{av}Ge, in units of 10^{12} dyn cm^{-2}.

Temperature (K)	C_{44}	C_{11}	C_{12}	B_0
0 (classical)	0.5893	1.3845	0.5104	0.8018
0 (quantum)	0.5879	1.3770	0.5045	0.7953
100 (quantum)	0.5878	1.3763	0.5040	0.7948
100 (expt.)	0.6820	1.3120	0.4930	0.7660
300 (quantum)	0.5867	1.3702	0.4996	0.7898
300 (expt.)	0.6710	1.2880	0.4830	0.7513
500 (quantum)	0.5852	1.3624	0.4939	0.7834

the value found from the change in the potential energy in a homogeneous deformation of the crystal.

The temperature dependence of the lattice parameter of ^{av}Ge obtained by the PIMC simulations and by the QHA is presented in Fig. 4 for both the classical and the quantum treatments of the Ge nuclei. The quasiharmonic results show an overall agreement with the PIMC data. However, a systematic deviation is appreciable as the temperature increases above 200 K. We note that the classical result is independent of the isotope mass. At 0 K, we see a non-negligible lattice expansion of about 0.006 Å obtained in the quantum simulation, with respect to the lattice parameter obtained in the classical limit ($a=5.648\,786$ Å). This effect is due to the anharmonicity of the zero-point motion. The dotted line is a fit to experimental data.[31] The comparison between the PIMC results and the experimental data deserves two comments. First, at low temperatures, the PIMC data differ from experiment by about 0.006 Å. The employed potential for Ge was parametrized[17] to reproduce the experimental lattice parameter at 0 K treating the nuclei as classical particles. Therefore, the deviation of the PIMC results from experiment is related to the quantum nature of the nuclei and the

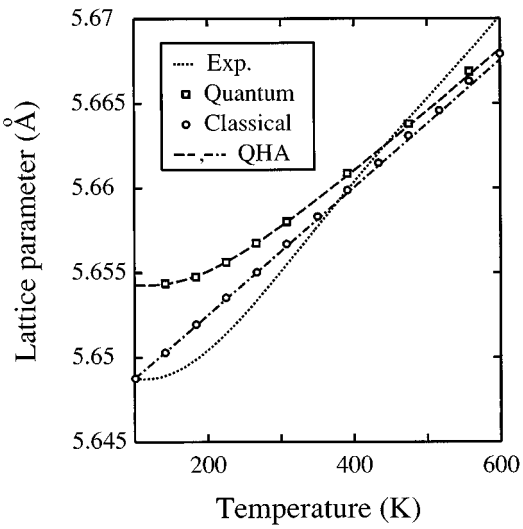

FIG. 4. Temperature dependence of the lattice parameter of ^{av}Ge. The dotted line corresponds to a fit to x-ray diffraction data (Ref. 31). The open squares are results from the quantum MC simulations. The circles are results of the classical MC simulation. The dashed and dash-dotted lines are results obtained in the quantum and classical quasiharmonic approximation, respectively.

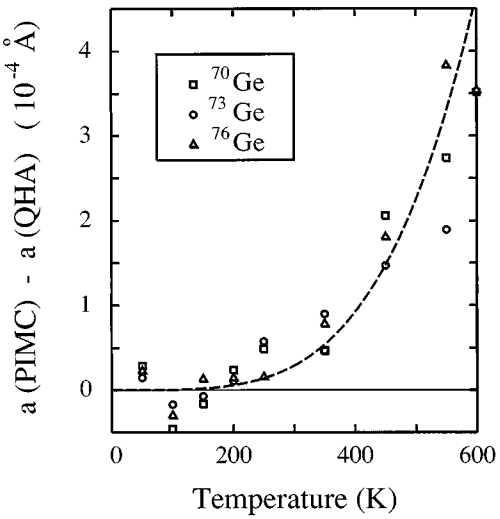

FIG. 5. Temperature dependence of the difference found between the lattice parameter obtained in the PIMC simulations and in the QHA. Results are shown for ^{70}Ge, ^{73}Ge, and ^{76}Ge. The dashed line is a guide to the eye.

anharmonicity of the interatomic potential. An improved parametrization of the potential would imply to fit, in the classical limit at 0 K, the equilibrium lattice parameter to a value about 0.006 Å smaller than the experimental one. Second, the employed potential predicts a thermal expansion of the Ge lattice smaller than the experimental one, as shown by the different slopes of the simulated and experimental curves in Fig. 4.

We turn now to compare the PIMC results with the QHA results in order to check the limitations of the QHA. We have found that the lattice parameters for the isotopically pure crystals obtained from the PIMC simulations are larger than those obtained from the QHA, and that this deviation goes up as temperature increases. This difference is shown in Fig. 5 for three isotopes: ^{70}Ge, ^{73}Ge, and ^{76}Ge. At $T=500$ K the deviation is about 2.5×10^{-4} Å, which is of the same order as the change in the lattice parameter due to the isotope mass (see below). The difference between the QHA and the PIMC results is due to anharmonic effects not taken into account in the QHA. The data in Fig. 5 show that these effects do not depend on the isotope mass and are significant above 200 K. Another evidence of anharmonic effects not included in the QHA can be obtained by plotting the potential–to–kinetic-energy ratio derived from the PIMC simulations vs. temperature. This ratio is shown in Fig. 6 for three isotopes: ^{70}Ge, ^{73}Ge, and ^{76}Ge. The energy ratio increases with temperature, departing appreciably from the value expected in a harmonic or quasiharmonic approximation, where it should be unity irrespective of temperature (virial theorem).

In the following, we present the results derived from the PIMC simulations and the QHA for the isotopic effect on the lattice constant of isotopically pure crystals. In the framework of the QHA of solids, the difference between the lattice parameters corresponding to an isotope mass M and the isotope ^{76}Ge (taken as reference) is given by[1,3]

$$a(^{M}\mathrm{Ge})-a(^{76}\mathrm{Ge})=C(T)[M^{-1/2}-{}^{76}M^{-1/2}], \qquad (4)$$

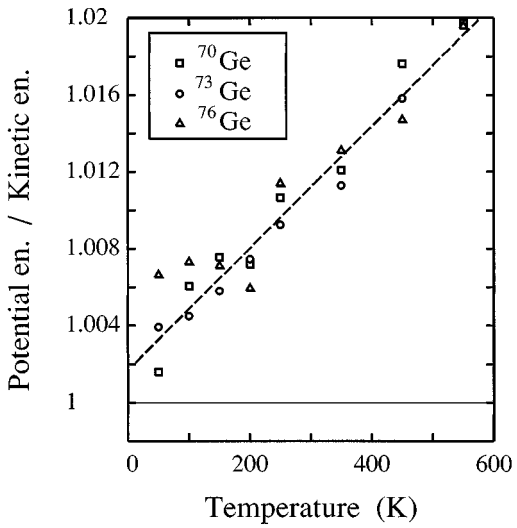

FIG. 6. Potential–to–kinetic-energy ratio obtained from the PIMC simulations vs temperature for ^{70}Ge,^{73}Ge, and ^{76}Ge. The dashed line is a guide to the eye. The continuous horizontal line represents the result expected in a harmonic or a quasiharmonic approximation.

where $C(T)$ is a temperature-dependent constant, and ^{76}M is the mass of the isotope ^{76}Ge. In Fig. 7, we show this lattice parameter increment for the different Ge isotopes versus the inverse square of the isotope mass for several temperatures, as derived from the PIMC simulations and the QHA. In this figure, the value of the lattice constant $a(^{76}\mathrm{Ge})$ taken as reference was obtained from a least-squares fit of the data $a(^{M}\mathrm{Ge})$, obtained for the different isotopes, to a linear equation $cM^{-1/2}+d$. In this way, the statistical noise in the subtraction of the left-hand side in Eq. (4) is reduced. Note that

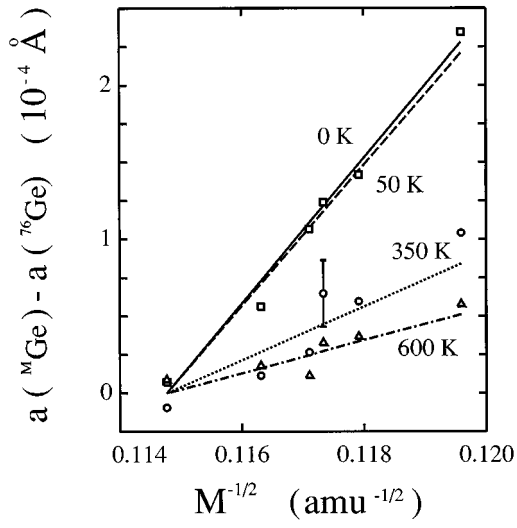

FIG. 7. Difference between the lattice parameter of the stable germanium isotopes and that of ^{76}Ge vs the inverse square of the isotope mass for different temperatures. Symbols are results from the quantum simulations: squares at 50 K, circles at 350 K, and triangles at 600 K. Lines are results from the quantum quasiharmonic approximation: continuous line at 0 K, dashed at 50 K, dotted at 350 K, and dash-dotted line at 600 K.

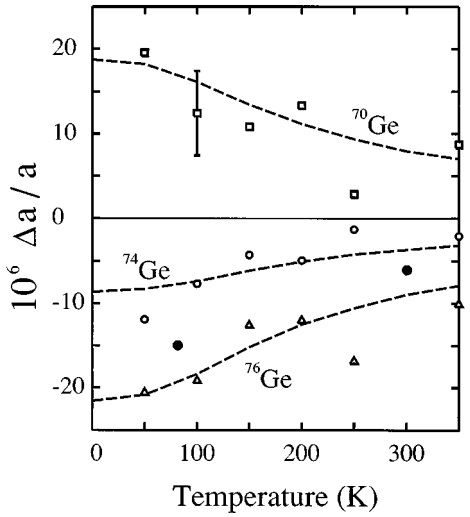

FIG. 8. Fractional change of the lattice parameter, $\Delta a/a$, vs temperature for three different germanium isotopes. Dashed lines are results obtained from the quantum quasiharmonic approximation. Open symbols represent PIMC simulation results: squares for ^{70}Ge, circles for ^{74}Ge, and triangles for ^{76}Ge. Solid circles are experimental results for ^{74}Ge (Ref. 5). The continuous horizontal line represents the classical limit ($\Delta a=0$).

the systematic deviation between the PIMC and QHA results for $a(^{M}\mathrm{Ge})$ found at temperatures above 200 K (see Fig. 4) does not depend on the isotope mass, and therefore it disappears in the subtraction given by Eq. (4). Within the statistical uncertainty of our simulation results, both PIMC and QHA data shown in Fig. 7 coincide. As expected, the maximum isotope effect on the lattice constant is obtained at $T=0$ K. Thus, from the results of the quasiharmonic approximation, the difference between the lattice parameters of ^{70}Ge and ^{76}Ge at $T=0$ K is found to be 2.3×10^{-4} Å. By fitting the results at $T=0$ (continuous line) to Eq. (4), we obtain $C(0)=0.047\,24$ Å amu$^{1/2}$. At this temperature, we checked that the extrapolation of this equation to infinite mass (classical limit) yields the same lattice parameter as that corresponding to the absolute minimum of the employed SW potential. As temperature increases, $C(T)$ in Eq. (4) (the slope of the lines in Fig. 7) decreases, since the system approaches the classical regime, in which the isotope mass effect disappears.

The fractional change of the lattice parameter with respect to $^{\mathrm{av}}$Ge, $\Delta a/a=[a(^{M}\mathrm{Ge})-a(^{\mathrm{av}}\mathrm{Ge})]/a(^{\mathrm{av}}\mathrm{Ge})$, for ^{70}Ge, ^{74}Ge, and ^{76}Ge, is presented in Fig. 8 in a temperature range between 0 and 350 K. Both PIMC and QHA results are identical within the statistical uncertainty of the simulation. As one goes to higher temperatures, the isotopic effect on the lattice parameter decreases, and the results converge to the horizontal thin line (zero fractional change in the lattice parameter). We show also the experimental data for ^{74}Ge obtained by Buschert *et al.*[5] at $T=78$ K and 300 K. A comparison of the experimental results with those obtained in the quantum QHA is given in Table III. The QHA results deviate by about 40% from experiment. We expect that the low values of the Grüneisen constants of the optical modes of Ge found for the SW-type potential are in part responsible for this deviation from experiment.[5,31,34] To check this point, we

TABLE III. Fractional change of the isotopic lattice parameter of ^{74}Ge, in units of 10^{-6}.

Temperature (K)	Expt. value	QHA
78	-14.9 ± 0.3	-8.9
300	-6.3 ± 0.3	-3.7

performed a QHA increasing the Grüneisen constants of the optical modes by 0.35. The deviation from experiment found for ^{74}Ge was then reduced by a factor of 2.

In the comparison between the simulation and QHA results with experiment, we made the approximation of treating natural Ge as ^{av}Ge, i.e., the atomic mass was set equal to the average mass of natural germanium. Another approximation to the lattice parameter of natural germanium is given by the average $\langle a \rangle$ of the lattice parameters of the pure isotope crystals weighted by their relative abundance. It is interesting to note that both results are different, giving $a(^{M}\mathrm{Ge}) < \langle a \rangle$. Thus, at $T=0$ K, the QHA result is $\langle a \rangle - a(^{M}\mathrm{Ge}) = 1.4\times10^{-6}$ Å. At $T=600$ K this value is reduced to $\langle a \rangle - a(^{M}\mathrm{Ge}) = 2\times10^{-7}$ Å. The results shown in Fig. 8 would change by less than 3% if we used $\langle a \rangle$ instead of $a(^{av}\mathrm{Ge})$ for defining the fractional change in the lattice parameter.

It is interesting to compare the QHA results with those obtained from a theoretical expression derived by Buschert *et al.*[5] for the fractional change in the lattice parameter at $T=0$:

$$\frac{\Delta a}{a} = -\frac{1}{B_0 a^3}\frac{\Delta M}{M}\left(\gamma_0 \hbar\omega_0 + \frac{3}{4}\gamma_a k_B \Theta_D\right), \tag{5}$$

where γ_0 and γ_a are the average Grüneisen constants for the optical and acoustic modes, respectively, B_0 is the bulk modulus at $T=0$ K, ω_0 is the frequency for the optical modes near the Γ point, and Θ_D is the Debye temperature of the crystal. This formula is a simplified QHA where it was assumed a Debye spectrum for the acoustic phonons and a constant frequency for the optical phonons. Using the experimental values for these parameters,[41] Buschert *et al.* obtained a fractional change of -12.0×10^{-6} for ^{74}Ge. If we use the values of $\gamma_0=0.85$, $\gamma_a=0.40$, $\hbar\omega_0=7.04\times10^{-14}$ erg, and $\Theta_D=310$ K (Ref. 42) obtained from our calculations, the result is $\Delta a/a=-9.0\times10^{-6}$, in close agreement with the value obtained from the QHA at 0 K of $\Delta a/a=-9.2\times10^{-6}$.

IV. SUMMARY

In this contribution we have calculated the lattice parameter for the five stable isotopes of *c*-Ge. This dependence on the isotope mass is directly related to the anharmonicity of the interatomic potentials and to the quantum nature of the nuclei (different zero-point energy for different isotope mass). The QHA fails to reproduce the MC simulation results as temperature rises, due to anharmonicities not included in this approximation. This translates into simulated lattice parameters shifted toward values higher than those obtained from the QHA, and a potential–to–kinetic energy ratio increasing with temperature. At $T=500$ K, this shift is about 2.5×10^{-4} Å, which is of the same order as the maximum isotope effect (2.3×10^{-4} Å), found at 0 K between ^{70}Ge and ^{76}Ge. At $T=500$ K the PIMC potential–to–kinetic-energy ratio is 1.02, i.e., higher than the value 1 corresponding to the QHA. Comparison of the isotopic effect found for the lattice parameter to experimental results shows a relatively good agreement, given the shortcomings described for the employed potential, especially for the Grüneisen constants of the optical modes, which are underestimated by about 25%.

ACKNOWLEDGMENTS

This work was supported by CICYT (Spain) under Contract No. PB93-1254. One of us (J.C.N.) thanks the Ministerio de Educación y Cultura (Spain) for financial support.

[1] A.A. Berezin and A. M. Ibrahim, Mater. Chem. Phys. **19**, 407 (1988).
[2] E. J. Covington and D. J. Montgomery, J. Chem. Phys. **27**, 1030 (1957).
[3] J. L. Anderson, J. Nasise, K. Philipson, and F. E. Pretzel, J. Phys. Chem. Solids **31**, 613 (1970).
[4] A. R. Ruffa, Phys. Rev. B **27**, 1321 (1983).
[5] R. C. Buschert, A. E. Merlini, S. Pace, S. Rodriguez, and M. H. Grimsditch, Phys. Rev. B **38**, 5219 (1988).
[6] H. Holloway, K. C. Hass, M. A. Tamor, T. R. Anthony, and W. F. Banholzer, Phys. Rev. B **44**, 7123 (1991).
[7] K. Itoh, W. L. Hansen, E. E. Haller, J. W. Farmer, V. I. Ozhogin, A. Rudnev, and A. Tikhomirov, J. Mater. Res. **8**, 1341 (1993).
[8] H. D. Fuchs, P. Etchegoin, M. Cardona, K. Itoh, and E. E. Haller, Phys. Rev. Lett. **70**, 1715 (1993).
[9] J. Spitzer, T. Ruf, M. Cardona, W. Dondl, R. Schorer, G. Abstreiter, and E. E. Haller, Phys. Rev. Lett. **72**, 1565 (1994).
[10] A. T. Collins, G. Davies, H. Kanda, and G. S. Woods, J. Phys. C **21**, 1363 (1988).
[11] T. R. Anthony, W. F. Banholzer, J. F. Fleischer, L. Wei, P. K. Kuo, R. L. Thomas, and R. W. Pryor, Phys. Rev. B **42**, 1104 (1990).
[12] A. T. Collins, S. C. Lawson, G. Davies, and H. Kanda, Phys. Rev. Lett. **65**, 891 (1990).
[13] P. Etchegoin, H. D. Fuchs, J. Weber, M. Cardona, L. Pintschovius, N. Pyka, K. Itoh, and E. E. Haller, Phys. Rev. B **48**, 12 661 (1993).
[14] M. H. Müser, P. Nielaba, and K. Binder, Phys. Rev. B **51**, 2723 (1995).
[15] J. L. Barrat, P. Loubeyre, and M. L. Klein, J. Chem. Phys. **90**, 5644 (1989).
[16] G. P. Srivastava, *The Physics of Phonons* (Adam Hilger, Bristol, 1990).
[17] K. Ding and H. C. Andersen, Phys. Rev. B **34**, 6987 (1986).
[18] M. Laradji, D. P. Landau, and B. Dünweg, Phys. Rev. B **51**, 4894 (1995). The parameters are $A=7.049\,556\,277$, $B=0.602\,224\,558$, $p=4$, $q=0$, $a=1.840$, $\lambda=31$, $\gamma=1.2$, $\epsilon=1.93$ eV, $\sigma=2.179\,120\,447$ Å.

[19] F. H. Stillinger and T. A. Weber, Phys. Rev. B **31**, 5262 (1985).
[20] M. J. Gillan, in *Computer Modelling of Fluids, Polymers, and Solids*, edited by C. R. A. Catlow, S. C. Parker, and M. P. Allen (Kluwer, Dordrecht, 1990); M. J. Gillan, Philos. Mag. A **58**, 257 (1988).
[21] D. M. Ceperley, Rev. Mod. Phys. **67**, 279 (1995).
[22] K. S. Schweizer, R. M. Stratt, D. Chandler, and P. G. Wolynes, J. Chem. Phys. **75**, 1347 (1981).
[23] R. Ramírez and C. P. Herrero, Phys. Rev. B **48**, 14 659 (1993).
[24] N. Metropolis, A. W. Rosenbluth, M. N. Rosenbluth, A. H. Teller, and E. Teller J. Chem. Phys. **21**, 1087 (1953).
[25] J. P. Valleau, in *Computer Simulation in Materials Science*, edited by M. Meyer and V. Pontikis (Kluwer, Dordrecht, 1991).
[26] K. Binder and D. W. Heermann, *Monte Carlo Simulation in Statistical Physics* (Springer, Berlin, 1988).
[27] J. C. Noya, C. P. Herrero, and R. Ramírez, Phys. Rev. B **53**, 9869 (1996).
[28] P. M. Morse, *Thermal Physics* (W.A. Benjamin, New York, 1964).
[29] N. W. Ashcroft and N. D. Mermin, *Solid State Physics* (Saunders College, Philadelphia, 1976).
[30] R. Ramírez and M. C. Böhm, Int. J. Quantum Chem. **34**, 571 (1988).
[31] *Physics of Group IV Elements and III-IV Compounds*, edited by O. Madelung, Landolt-Börnstein, New Series, Group III, Vol. 17a (Springer, Berlin, 1982).
[32] P. Giannozzi, S. de Gironcoli, P. Pavone, and S. Baroni, Phys. Rev. B **43**, 7231 (1991).
[33] G. Nellin and G. Nilsson, Phys. Rev. B **5**, 3151 (1972).
[34] J. B. Renucci, M. A. Renucci, and M. Cardona, Solid State Commun. **9**, 1651 (1971).
[35] R. R. Reeber, Phys. Status Solidi A **32**, 321 (1975).
[36] C. H. Xu, C. Z. Wang, C. T. Chan, and K. M. Ho, Phys. Rev. B **43**, 5024 (1991).
[37] P. Pavone, K. Karch, O. Schütt, W. Windl, D. Strauch, P. Giannozzi, and S. Baroni, Phys. Rev. B **48**, 3156 (1993).
[38] P. N. Keating, Phys. Rev. **145**, 637 (1966).
[39] B. Dünweg and D. P. Landau, Phys. Rev. B **48**, 14 182 (1993).
[40] C. Kittel, *Introduction to Solid State Physics*, 3rd ed. (Wiley, New York, 1967).
[41] The values used in Ref. 5 are $B_0 = 0.775 \times 10^{12}$ dyn/cm^2, $\gamma_0 = 1.12$, $\gamma_a = 0.40$, $\Theta_D = 374$ K, $\hbar\omega_0 = 5.97 \times 10^{-14}$ erg.
[42] The value of the Debye temperature was obtained from the results of the QHA by fitting the heat capacity at low temperatures to a T^3 law.